



**HAL**  
open science

## Iron borate films: Synthesis and characterization

S Yagupov, M Strugatsky, K Seleznyova, Yu Mogilenec, E Milyukova, E Maksimova, I Nauhatsky, A Drovosekov, N Kreines, Janis Kliava

► **To cite this version:**

S Yagupov, M Strugatsky, K Seleznyova, Yu Mogilenec, E Milyukova, et al.. Iron borate films: Synthesis and characterization. *Journal of Magnetism and Magnetic Materials*, 2016, 417, pp.338 - 343. 10.1016/j.jmmm.2016.05.098 . hal-01392749

**HAL Id: hal-01392749**

**<https://hal.science/hal-01392749>**

Submitted on 4 Nov 2016

**HAL** is a multi-disciplinary open access archive for the deposit and dissemination of scientific research documents, whether they are published or not. The documents may come from teaching and research institutions in France or abroad, or from public or private research centers.

L'archive ouverte pluridisciplinaire **HAL**, est destinée au dépôt et à la diffusion de documents scientifiques de niveau recherche, publiés ou non, émanant des établissements d'enseignement et de recherche français ou étrangers, des laboratoires publics ou privés.



Distributed under a Creative Commons Attribution - ShareAlike 4.0 International License

# Iron borate films: Synthesis and characterization

S. Yagupov<sup>a</sup>, M. Strugatsky<sup>a,\*</sup>, K. Seleznyova<sup>a,b</sup>, Yu. Mogilenec<sup>a</sup>, E. Milyukova<sup>a</sup>,  
E. Maksimova<sup>a</sup>, I. Nauhatsky<sup>a</sup>, A. Drovosekov<sup>c</sup>, N. Kreines<sup>c</sup>, J. Kliava<sup>b</sup>

<sup>a</sup> Physics and Technology Institute, Crimean Federal V.I. Vernadsky University, 4 Vernadsky Avenue, Simferopol 295007, Russia

<sup>b</sup> LOMA, UMR 5798 Université de Bordeaux-CNRS, 33405 Talence cedex, France

<sup>c</sup> P.L. Kapitza Institute for Physical Problems RAS, 2 ul. Kosygina, Moscow 119334, Russia

---

## A B S T R A C T

### Keywords:

Iron borate film  
Liquid phase epitaxy  
Electron microscopy  
Energy-dispersive spectroscopy  
X-ray diffraction  
Electron magnetic resonance

We report the first successful synthesis of iron borate films. FeBO<sub>3</sub> films on GaBO<sub>3</sub> single crystal substrates have been prepared by a liquid phase epitaxy route. In order to determine optimal crystallization regimes, a series of experiments has been carried out. Electron microscope studies have allowed monitoring different phases of the film formation. The compositions of the film and of the substrate have been determined by energy dispersive spectroscopy. X ray diffraction analysis has allowed an accurate determination of a mismatch between the lattice parameters of the film and of the substrate. Electron magnetic resonance studies of the FeBO<sub>3</sub> film confirm the existence of magnetic ordering. The values of the effective Dzyaloshinskii field as well as the Néel temperature are in good accordance with those previously determined for FeBO<sub>3</sub> single crystal.

---

## 1. Introduction

The research interest in iron borate FeBO<sub>3</sub> is mainly due to its remarkable magnetic, magneto acoustical, optical, magneto optical, resonance, etc., characteristics, e.g., see [1–6]. In particular, iron borate can be categorized as a “transparent magnet”, combining transmission windows in visible spectral range with room temperature magnetic ordering. From the standpoint of magnetic properties, FeBO<sub>3</sub> is an easy plane antiferromagnet with weak ferromagnetism and the Néel temperature  $T_N \approx 348$  K. The AFMR studies of FeBO<sub>3</sub> were carried out in a wide range of temperatures and frequencies [6]. From the standpoint of crystalline structure, FeBO<sub>3</sub> is a rhombohedral calcite type crystal of space group  $D_{3d}^6$  [7].

In contrast to conventional ferromagnets, in iron borate the surface magnetocrystalline anisotropy, caused by symmetry breaking in the surrounding of near surface iron ions [8], is not suppressed. This is due to the fact that the demagnetizing field, proportional to weak ferromagnetic vector, is small and the anisotropy in the basal plane, (0001) in hexagonal coordinate system, is weak [7]. Consequently, the magnetic characteristics of a thin (0.01–0.1 μm) near surface layer of iron borate drastically differ from those in the volume. Such effects were studied both

experimentally using magneto optic Kerr effect [9] and theoretically [9,10]. Another interesting effect is that surface magneto crystalline anisotropy stimulates the formation of bubble magnetic domains in the near surface layer of iron borate [9]. From the standpoint of practical applications, the surface of iron borate single crystals can be considered as a magnetic memory element analogous to thin film magnetic materials containing cylindrical magnetic domains. Undoubtedly, thin FeBO<sub>3</sub> magnetic films deposited on a diamagnetic transparent substrate are appropriate for studying surface magnetism using not only the Kerr effect [9] but also the Faraday effect. In particular, in very thin (less than 0.1 μm) iron borate films one can study “pure” surface magnetic effects, not altered by volume magnetism.

In FeBO<sub>3</sub> single crystals having the shape of basal plates, interesting magneto acoustic effects were found, related to magnetic structure of this crystal [2,11]. The magnetization in this case follows quasi statically natural longitudinal [2] and transversal [11] acoustic modes. In very thin FeBO<sub>3</sub> film, one can expect the emergence of forced magnetic oscillations at frequencies approaching the natural magnetic oscillation frequency, i.e. the AFMR frequency, resulting in promising new effects.

The aim of the present work is to develop the synthesis technique, to obtain and to characterize FeBO<sub>3</sub> films on a diamagnetic substrate. As the substrate we have used gallium borate, GaBO<sub>3</sub>, single crystal. This material is isostructural with FeBO<sub>3</sub>; besides, it is also transparent in the visible range, albeit diamagnetic [12]. Both crystals have similar lattice parameters: in iron borate

---

\* Corresponding author.

E-mail address: [strugatsky@crimea.edu](mailto:strugatsky@crimea.edu) (M. Strugatsky).

$a=4.626$ ,  $c=14.493$ , and in gallium borate  $a=4.568$ ,  $c=14.182$  Å (in the hexagonal coordinate system). As one can see, the relative difference between the corresponding parameters for both crystals is less than 2%, while the structure of deposited film is known to reproduce that of substrate if this difference does not exceed ca. 14% [13]. Thus,  $\text{GaBO}_3$  crystal seems to be the best candidate to be used as substrate for depositing  $\text{FeBO}_3$  film.

A successful depositing of a high quality film requires using a high quality substrate. On the basis of our previous studies on synthesis of iron based borate crystals, e.g., see [12,14], we have concluded that high quality samples can be obtained by the solution in the melt technique. Thus, this technique has been used for synthesizing the substrate, and for depositing the  $\text{FeBO}_3$  film in these conditions, the liquid phase epitaxy (LPE) technique appears to be optimal.

During the sample synthesis, different phases of the film for formation and compositions of the film and the substrate have been monitored by electron microscopy and energy dispersive spectroscopy (EDS), respectively. The lattice parameters of the film and of the substrate have been measured by X ray diffraction (XRD). The magnetic characteristics of the film, such as the Dzyaloshinskii field  $H_D$  and  $T_N$ , have been determined by means of electron magnetic resonance (EMR).

## 2. Synthesis of the film

The synthesis of  $\text{FeBO}_3$  film by the LPE technique includes the following steps:

- (i) Choosing appropriate charge compositions and temperature modes;
- (ii) Preparing a high quality  $\text{GaBO}_3$  substrate;
- (iii) LPE synthesis of the  $\text{FeBO}_3$  film on the substrate.

The crystallizations in the steps (ii) and (iii) were carried out with  $\text{Ga}_2\text{O}_3$   $\text{B}_2\text{O}_3$   $\text{PbO}$   $\text{PbF}_2$  and  $\text{Fe}_2\text{O}_3$   $\text{B}_2\text{O}_3$   $\text{PbO}$   $\text{PbF}_2$  solution melts, respectively. The most appropriate charge compositions, determined by differential thermal analysis method, are shown in Table 1 [12,14].

The synthesis of the  $\text{GaBO}_3$  single crystal the substrate has recently been described by some of the present authors [12].

The synthesized  $\text{GaBO}_3$  crystals are shown in Fig. 1. For comparison, we also show previously synthesized  $\text{FeBO}_3$  single crystals [14]. Both  $\text{GaBO}_3$  and  $\text{FeBO}_3$  crystals have the shape of hexagonal plates with the dimensions of 3–7 mm in the basal plane and 0.05–0.1 mm in thickness. Note that gallium borate is colorless while iron borate is green.

The operating mode used to deposit  $\text{FeBO}_3$  film by the LPE route was as follows: the  $\text{GaBO}_3$  substrate was placed into a metallic supporting cone perforated with small holes and maintained during 30 min in a crucible containing the solution melt for  $\text{FeBO}_3$  synthesis, see Table 1. The corresponding temperature mode is shown in Fig. 2. It includes the following stages: (i) heating of the furnace, (ii) homogenization of the solution melt, (iii) fast temperature dropping in order to avoid the emergence of spurious phases, e.g.,  $\text{Fe}_3\text{BO}_6$ , (iv) nucleation and film growth and

**Table 1**  
Charge compositions (in mass %) used for synthesizing  $\text{GaBO}_3$  substrate and  $\text{FeBO}_3$  film.

	$\text{Ga}_2\text{O}_3$	$\text{Fe}_2\text{O}_3$	$\text{B}_2\text{O}_3$	$\text{PbO}$	$\text{PbF}_2$
$\text{GaBO}_3$ substrate	18.6	0	42.4	27.3	11.7
$\text{FeBO}_3$ film	0	5.8	51.2	29.3	13.7

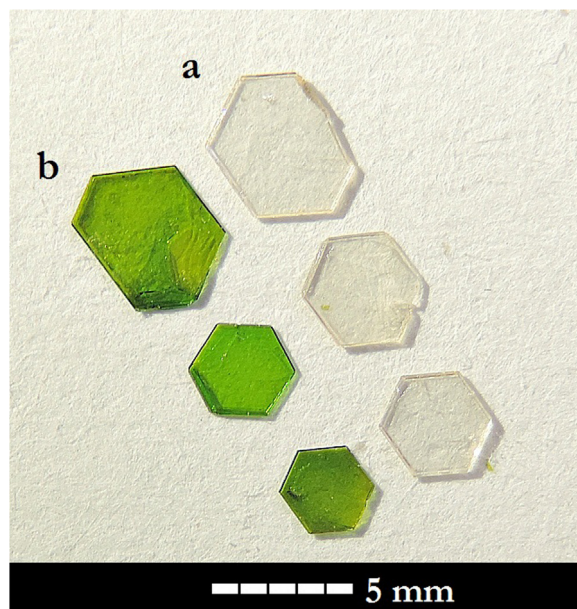


**Fig. 1.**  $\text{GaBO}_3$  (a) and  $\text{FeBO}_3$  (b) single crystals synthesized by solution in the melt technique. (For interpretation of the references to color in this figure, the reader is referred to the web version of this article.)

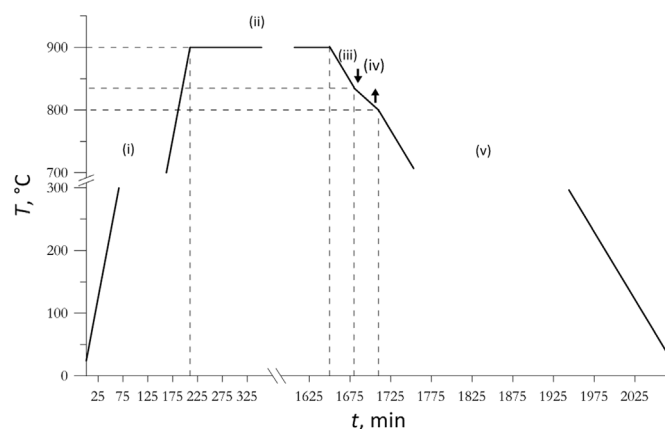


**Fig. 2.** Temperature mode used in synthesizing  $\text{FeBO}_3$  film, see the text for details.

(v) cooling the furnace. The moments when the cone with the substrate has been immersed in and extracted from the solution melt are indicated by arrows. Due to the perforation, during the immersion the solution melt was filling the cone and bathing the whole substrate. During the extraction, the solution melt was withdrawn through the holes back into the crucible, and the synthesized sample (substrate with deposited film) remained in the cone, see Fig. 3. As one can see in online version, after the crystallization the sample surface becomes light green, as characteristic of iron borate.

## 3. Characterization of the synthesized samples

### 3.1. Electron microscopy

$\text{FeBO}_3$  film formation has been monitored by electron microscopy using REM 106 and field emission SEM JSM 7800F microscopes.

The film formation in this system occurred following the epitaxial island growth mechanism. Consecutive stages of the film growth are shown in Fig. 4. Conventionally, it can be divided into

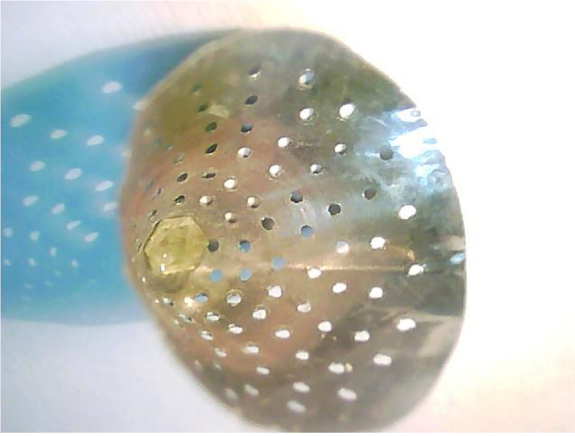


**Fig. 3.** Synthesized sample in the supporting cone. The diameter of the cone basis is ca. 15 mm and those of the holes are ca. 0.5 mm.

four stages: (a) formation of film islands, (b) coalescence of the islands with formation of canals, (c) coalescence of fragments of the film and filling the canals in and (d) formation of a continuous film.

**Fig. 5** shows: (a) nucleation centers of  $\text{FeBO}_3$  on  $\text{GaBO}_3$  substrate and (b) a coalescence of these centers, constituting a fragment of well formed film. From **Figs. 4** and **5** it is obvious that all nucleation centers have the same orientation on  $\text{GaBO}_3$  surface; thus, the structure of  $\text{FeBO}_3$  film replicates that of  $\text{GaBO}_3$  substrate.

The developed technique allows synthesizing  $\text{FeBO}_3$  films of

different thickness, including those suitable for studying surface magnetism.

### 3.2. Energy dispersive spectroscopy studies

The compositions of the film and the substrate have been locally determined by EDS with X Max silicon drift X ray detector of JSM 7800F microscope. Data have been acquired at a low acceleration voltage of 2 kV. A super hybrid lens with gentle beam produced large probe current at low voltage enabling an express analysis of dielectric structures.

**Fig. 6** shows EDS spectra of a sample with partly deposited film, corresponding to the stage shown in **Fig. 4(b)**. If the electron beam is focused on the surface of the substrate, see **Fig. 6(a)**, the EDS spectrum shows lines arising from boron, oxygen, gallium and iron. In this case, the iron line is due to iron borate nucleation centers of nanometric size. Otherwise, if the electron beam is focused on the surface of the film, see **Fig. 6(b)**, the line arising from gallium vanishes. Therefore, we confirm that we are indeed dealing with  $\text{FeBO}_3$  layer deposited on the substrate.

### 3.3. XRD studies

The XRD studies of the synthesized samples have been carried out with X ray diffractometer using a monochromatic  $K_{\alpha 1}$  copper radiation of 1.54051 Å wavelength. The lattice parameters  $c$  have been calculated using the following expression [15]:

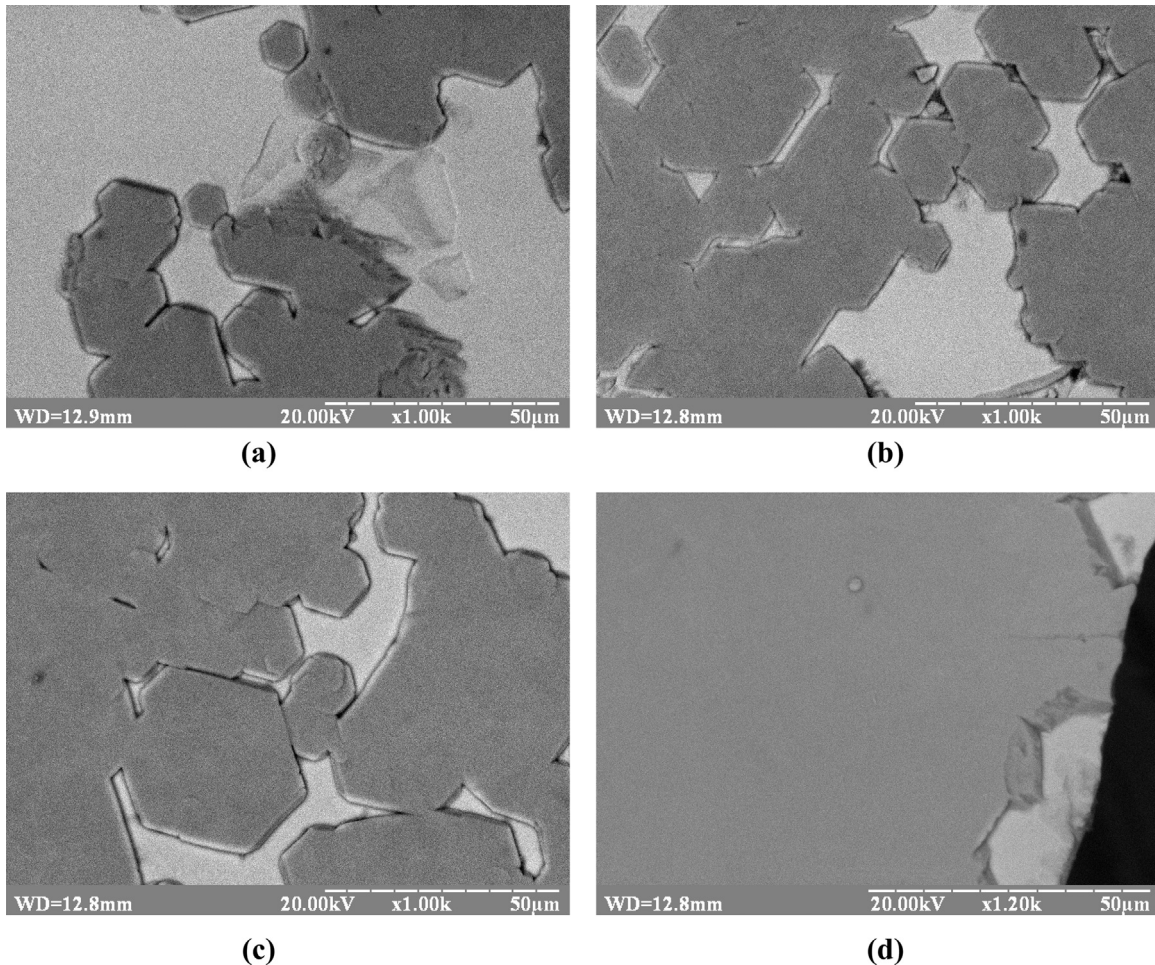


**Fig. 4.** Electron microscope pictures taken with REM 106, showing different stages of  $\text{FeBO}_3$  film formation, see the text for details.

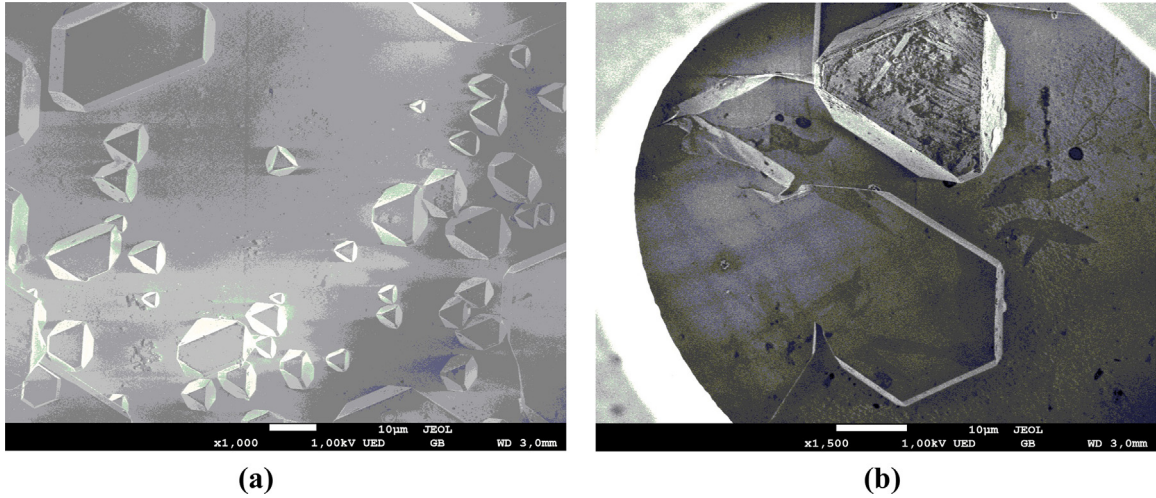


**Fig. 5.** Electron microscope pictures taken with a field emission SEM JSM-7800F microscope, showing FeBO<sub>3</sub> film on GaBO<sub>3</sub> substrate for two different magnifications.

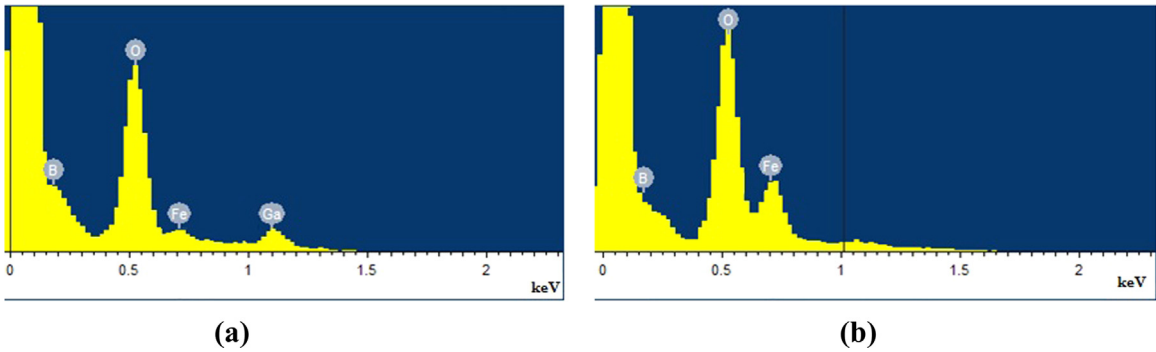


**Fig. 6.** EDS spectra of a typical sample. The electron beam is focused on the surface of the substrate (a) or on that of the film (b).

$$\frac{1}{d^2} = \frac{4}{3} \frac{h^2 + hk + k^2}{a^2} + \frac{l^2}{c^2} \quad (1)$$

where  $h$ ,  $k$  and  $l$  are Miller indices of a Bragg plane and  $d$  is the interplanar spacing calculated by means of Bragg's formula

$$2d \sin \vartheta = n\lambda \quad (2)$$

where  $\vartheta$  is the scattering angle,  $\lambda$  is the radiation wavelength and  $n$  is the reflection order. Thus, for the reflection peaks from the (00 $l$ ) planes ( $h = 0$  and  $k = 0$ ) Eq. (1) reduces to

$$c = dl. \quad (3)$$

For the determination of  $c$  in the film and in the substrate reflections from the plane with  $l = 12$  have been used. Fig. 7 shows XRD patterns for a synthesized sample as well as for FeBO<sub>3</sub> and GaBO<sub>3</sub> single crystals. From the XRD patterns of the single crystals, containing only one line, we get  $c = 14.476 \pm 0.017$  and  $c = 14.183 \pm 0.016$  Å for FeBO<sub>3</sub> and GaBO<sub>3</sub>, respectively. From the XRD pattern of the synthesized sample, containing lines arising both from the film and the substrate, we get  $c = 14.479 \pm 0.017$  and  $c = 14.182 \pm 0.016$  Å for the former and for the latter, respectively. The value of  $c$  for the film is in a good accordance with that for FeBO<sub>3</sub> single crystal, as expected for a FeBO<sub>3</sub> layer on the GaBO<sub>3</sub> substrate. One can see that the mismatch between the  $c$  values in the film and in the substrate is  $\Delta c = 0.297 \pm 0.034$  Å.

#### 3.4. EMR studies: magnetic properties of the film

The EMR studies of synthesized samples with relatively thick (ca. 4 μm) deposited film as well as of an iron borate single crystal have been carried out with laboratory developed spectrometer in

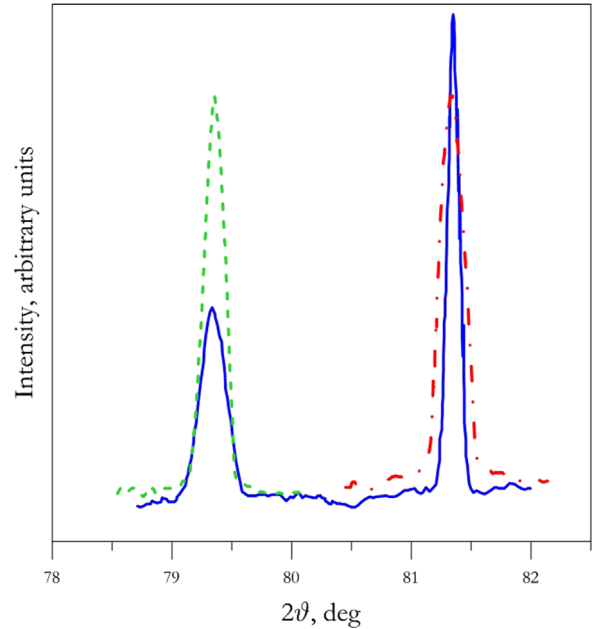


**Fig. 7.** XRD pattern of a synthesized sample (continuous, blue online) compared to those of FeBO<sub>3</sub> (dashed, green online) and GaBO<sub>3</sub> single crystals (dash-dotted, red online). (For interpretation of the references to color in this figure legend, the reader is referred to the web version of this article.)

the frequency range from 15.0 to 35.7 GHz, the temperature range from 293 to 350 K and the magnetizing field  $H$  up to 10 kOe applied in the basal plane of the sample. To detect the EMR signal,

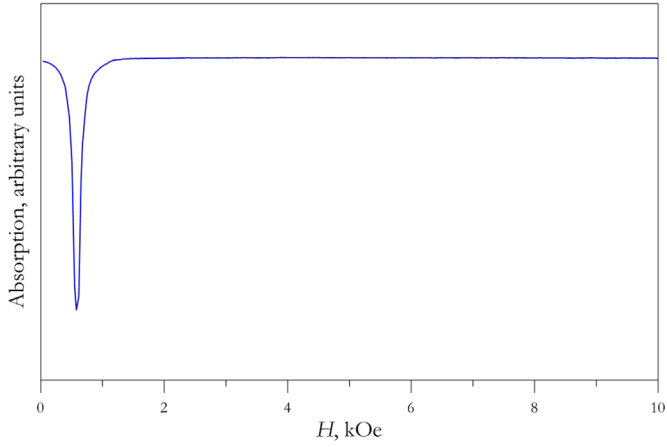


**Fig. 8.** EMR spectrum of  $\text{FeBO}_3$  single crystal at 17GHz and 293 K. The magnetizing field is applied in the basal plane.

the field dependence of the microwave power transmitted through the microwave cavity with the sample was measured.

First, we have carried out EMR studies of  $\text{FeBO}_3$  single crystal. Fig. 8 shows the EMR spectrum; obviously, only one resonance line is observed. Below  $T_N$ , this line has been identified as low frequency AFMR mode, e.g., see [6]. No other resonances occur in the temperature range from 4 to 293 K.

In contrast, the EMR spectra of the synthesized sample exhibit two resonance lines (see Fig. 9). The low field line occurs in the same magnetic field range as the AFMR line in  $\text{FeBO}_3$  single crystal; moreover, similarly to the latter line it undergoes a temperature dependent shift and disappears at ca. 350 K, in the vicinity of  $T_N$  for  $\text{FeBO}_3$  single crystals. Thus, this line can be identified as AFMR in  $\text{FeBO}_3$  film. The fact that this line is much broader in film than in single crystal can be explained by structural inhomogeneity and internal stresses in the film resulting in statistical distributions of spectroscopic parameters and, consequently, of the resonance fields. The high field line with the effective  $g$  factor  $g \approx 2$  appears not only above but also below  $T_N$ , though in

the latter case it is much weaker than the AFMR line. The occurrence of this line below  $T_N$  can be due to iron borate nanoclusters in the transition layer between the substrate and the film. Indeed, as local iron concentration in this layer is inhomogeneously distributed, such clusters are expected to be formed and give rise to cluster magnetic resonance.

The above identification can be corroborated by our recent EMR studies of mixed iron gallium borate,  $\text{Fe}_x\text{Ga}_{1-x}\text{BO}_3$ , single crystals ( $0.2 \leq x \leq 1$ ) in a broad temperature range, in which case we have also observed two resonance lines similar to those described here for  $\text{FeBO}_3$  film on  $\text{GaBO}_3$  substrate. A detailed account of the results for the mixed borate crystals will be published elsewhere. Here we mention only the interesting fact that in these crystals the intensity of the  $g \approx 2$  line does *not* follow the  $1/T$  Curie law, therefore it cannot be a usual paramagnetic resonance line; rather, it can also be due to iron borate nanoclusters.

From field swept EMR spectra recorded at different microwave frequencies, the dependence of the AFMR frequency on the magnetizing field (Dependence of Frequency on Field, DFF) can be obtained. Fig. 10 shows this dependence for  $\text{FeBO}_3$  film at different temperatures. In the case where  $H$  is applied in the basal plane, the low frequency AFMR mode is expressed as [6]:

$$\nu = \gamma \left[ H(H + H_D) + H_K^2 \right]^{1/2} \quad (4)$$

where  $\gamma$  is the gyromagnetic ratio for the free electron  $g$  value,  $g \approx 2.00$ ,  $H_D$  is the Dzyaloshinskii field and  $H_K^2$  is the isotropic energy gap. (An anisotropic part in the right hand side of Eq. (4) is neglected because for  $\text{FeBO}_3$  single crystal at room temperature the magnetocrystalline anisotropy in the basal plane is almost absent [16].)

From fitting the DFF for  $\text{FeBO}_3$  film at different temperatures  $H_D$  and  $H_K^2$  have been obtained and listed in Table 2. The  $H_D$  values are in a good accordance with those previously reported for  $\text{FeBO}_3$  single crystal at 300 K [6]. In contrast,  $H_K^2$  for  $\text{FeBO}_3$  film turns out to be several times larger than for  $\text{FeBO}_3$  single crystal. As far as elastic and magnetoelastic interactions influence the isotropic energy gap [6,17], this discrepancy can be ascribed to the

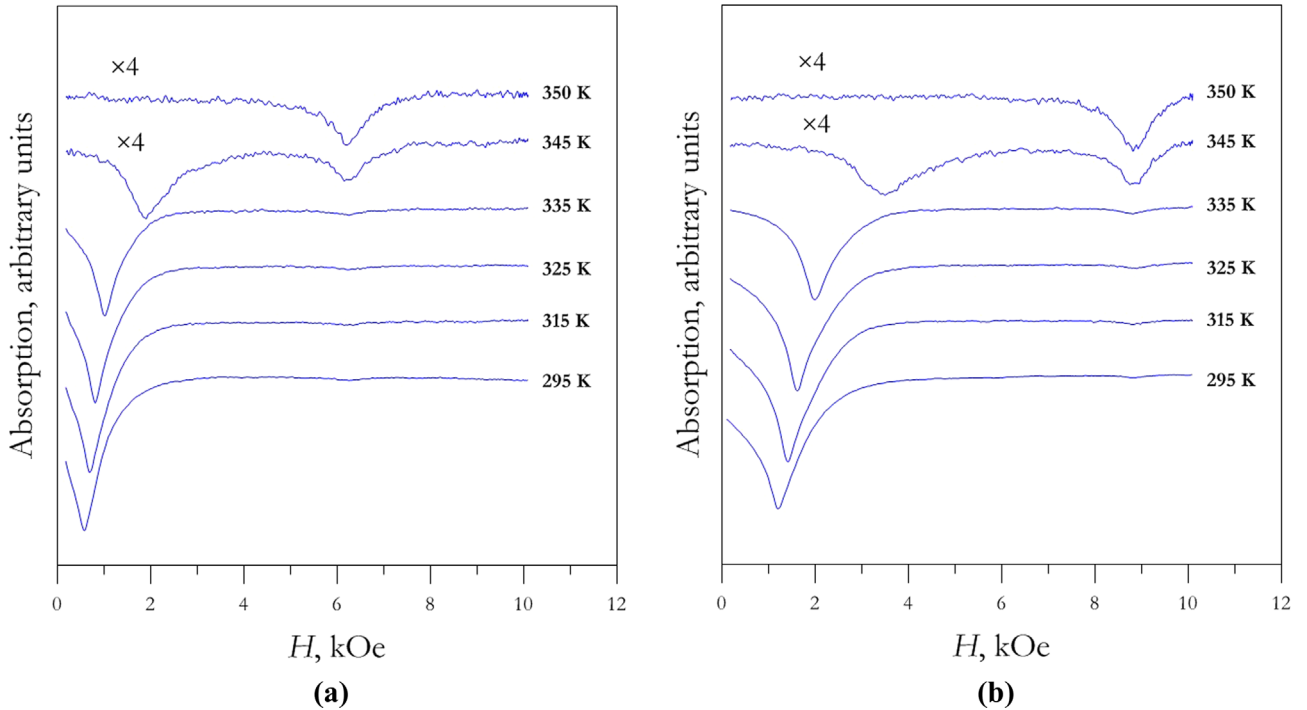


**Fig. 9.** EMR spectra series for the synthesized sample at  $\nu \approx 17$  (a) and 24.5 GHz (b) and different temperatures shown alongside the curves.

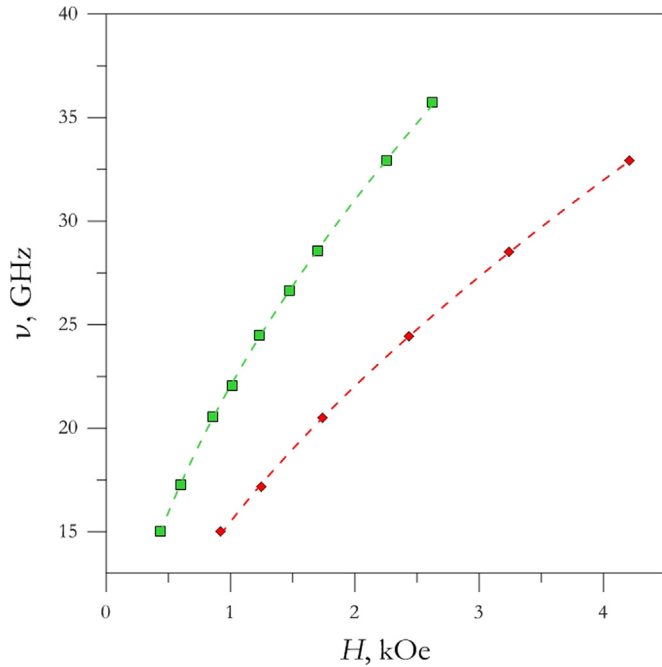


**Fig. 10.** Dependence of the AFMR frequency on the magnetizing field for FeBO<sub>3</sub> film at 300 (squares, green online) and 340 (diamonds, red online) K. The dashed curves are fittings according to Eq. (4). (For interpretation of the references to color in this figure legend, the reader is referred to the web version of this article.)

**Table 2**

$H_D$  and  $H_K^2$  in iron borate determined from AFMR studies.

T, K	Film, this work		Single crystal [6]	
	$H_D$ , kOe	$H_K^2$ , kOe <sup>2</sup>	$H_D$ , kOe	$H_K^2$ , kOe <sup>2</sup>
300	$57.7 \pm 0.3$	$3.3 \pm 0.3$	$62.0 \pm 0.5$	$0.6 \pm 0.5$
340	$28.3 \pm 0.2$	$1.3 \pm 0.4$		

mismatch of the lattice parameters in the film and in the substrate, *vide supra*.

In summary, the EMR studies confirm the existence of magnetic ordering in iron borate film.

#### 4. Conclusions

We have developed a suitable synthesis technique and prepared FeBO<sub>3</sub> films on GaBO<sub>3</sub> substrates by LPE route. Temperature modes used in synthesizing the film and the substrate have been experimentally determined. The developed technique allows obtaining films of different thickness, appropriate for magneto optical and magneto acoustical studies.

Various stages of the film formation have been monitored by electron microscopy, and the compositions of the film and the substrate have been controlled locally by EDS. The XRD studies have allowed determining the lattice parameter  $c$  for both the film and the substrate. These studies have confirmed that the synthesized samples are composed of FeBO<sub>3</sub> layer on GaBO<sub>3</sub> substrate.

The EMR studies have confirmed the existence of anti ferromagnetic ordering in 4  $\mu\text{m}$  FeBO<sub>3</sub> film, the Néel temperature being in a good accordance with that for FeBO<sub>3</sub> single crystal. Besides, these studies suggest that magnetically ordered nanoclusters are formed in the transition layer between the film and the substrate. The effective Dzyaloshinskii field and isotropic energy gap in FeBO<sub>3</sub> film at 300 and 340 K have been determined from fitting DFF data. The effective Dzyaloshinskii field values are close to those previously determined for FeBO<sub>3</sub> single crystal. However, the isotropic energy gap at 300 K in the film is several times larger than in single crystal; we ascribe this difference to a mismatch between the lattice parameters in the film and in the substrate.

In summary, in this work a new magnetic material, FeBO<sub>3</sub> thin film promising for studying surface magnetism as well as for practical applications as a memory element has been synthesized for the first time, to the best of our knowledge, and its magnetic characteristics have been described.

#### Acknowledgments

This work was partially supported by the Russian Foundation for Basic Research and the Ministry of Education, Science and Youth of the Republic of Crimea, in the framework of scientific project Grant no. 15 42 01008 “p\_ror\_a”.

The authors are grateful to S.A. Smagulova and her group from the Academic Technologic Laboratory “Graphene Nanotechnologies” of the North Eastern Federal University (Yakutsk), for the opportunity of using a JSM 7800F electronic microscope.

#### References

- [1] M. Eibshutz, M.E. Lines, Phys. Rev. B 7 (1973) 4907.
- [2] D. Afanasiev, I. Razdolski, K.M. Skibinsky, D. Bolotin, S.V. Yagupov, M. B. Strugatsky, A. Kirilyuk, Th Rasing, A.V. Kimel, Phys. Rev. Lett. 112 (2014) 147403.
- [3] M.B. Strugatsky, K.M. Skibinsky, V.V. Tarakanov, V.I. Khizhnyi, JMMM 241 (2002) 330.
- [4] A.V. Malakhovskii, I.S. Edelman, Phys. Status Solidi (b) 74 (1976) K145.
- [5] W. Jantz, J.R. Sandercock, W. Wetling, J. Phys. C 9 (1976) 2229.
- [6] L.V. Velikov, A.S. Prokhorov, E.G. Rudashevskii, V.N. Seleznev, Sov. Phys. JETP 39 (1974) 909.
- [7] R. Diehl, W. Jantz, B. I. Nolang, W. Wetling, Current Topics in Materials Science, E Kaldis (Ed.), Elsevier, New-York, 1984, vol. 11, pp. 241.
- [8] L. Néel, J. Phys. Radium 15 (1954) 225.
- [9] V.E. Zubov, G.S. Krinchik, V.N. Seleznyov, M.B. Strugatsky, JMMM 86 (1990) 105.
- [10] E.M. Maksimova, I.A. Nauhatsky, M.B. Strugatsky, V.E. Zubov, JMMM 322 (2010) 477.
- [11] Yu.N. Mitsay, K.M. Skibinsky, M.B. Strugatsky, A.P. Korolyuk, V.V. Tarakanov, V. I. Khizhnyi, JMMM 219 (2000) 340.
- [12] S. Yagupov, M. Strugatsky, K. Seleznyova, E. Maksimova, I. Nauhatsky, V. Yagupov, E. Milyukova, J. Kliava, Appl. Phys. A 121 (2015) 179.
- [13] L.I. Maissel, R. Glang, Hand Book of Thin Film Technology, McGraw Hill Book co, New York, 1970.
- [14] M.B. Strugatsky, S.V. Yagupov, Scientific Notes of Taurida National University, Ser. Phys. 19 (58) (2006) 76.
- [15] H. Lipson, H. Stipl, Interpretation of the Powder X-ray Patterns, Macmillan, London and St. Martins Press, New York, 1970.
- [16] D. Doroshev, I.M. Krygin, S.N. Lukin, A.N. Molchanov, A.D. Prokhorov, V. V. Rudenko, V.N. Seleznev, JETP Lett. 29 (1979) 257.
- [17] A.S. Borovik-Romanov, E.G. Rudashevskii, Sov. Phys. JETP 20 (1965) 1407.